CHAPTER IV
EVALUATION OF MECHANICAL RHEOLOGICAL AND THERMAL PROPERTIES OF POLY(TRIMETHYLENE TEREPHTHALATE)(PTT)/POLYETHYLENE BLEND USING COMPATIBILIZER BASED ON CARBOXYLATE AND IONOMER FOR AUTOMOTIVE APPLICATION

4.1 Abstract

Polymer blending is one way for development of new materials with excellent properties. In this study, poly(trimethylene terephthalate) (PTT) and polyethylene blended with maleic anhydride grafted high-density polyethylene (MAH–g–HDPE) and ethylene-methacrylic acid neutralized sodium metal (Na-EMAA), were used as compatibilizers. The blends were prepared by a twin-screw extruder with different ratios of polymers (PTT/HDPE and PTT/LLDPE: 80/20 and 60/40) and compatibilizers (0, 0.1, 0.5, 1, and 5 phr). The blends were characterized on mechanical, rheological, thermal, and morphological properties. By adding the compatibilizers, Young's modulus and tensile strength, impact strength and viscosity of the blends increased and smaller dispersed droplet size micrographs were observed. For the types of compatibilizers, MAH-g-HDPE and Na-EMAA, effected on mechanical properties. The melting and crystallization behavior of the blends also depended on type of compatibilizer.

Keywords: Poly(trimethylene terephthalate), Polyethylene, compatibilizer, polymer blend.

4.2 Introduction

Poly(trimethylene terephthalate) (PTT), a linear aromatic polyester was first synthesized by Whinfield and Dickson in 1941 (Rex *et al.*, 1949). PTT's properties are between poly(ethylene terephthalate) (PET) and poly(butylene terephthalate) (PBT) and it offers several advantageous properties. These are good strength and stiffness, good surface appearance, low shrinkage and warpage, good dimensional stability, outstanding elastic, recovery, and dyeability, which make it can use as applications such as carpets, textile fiber, automotive applications, or as an engineering plastic. However, it has low impact strength at low temperature which is the problems in the automotive applications (Run *et al.*, 2012). Thus, the modification of PTT with the other kind of polymers or polymer blend is one way to develop new material with excellence properties (Koning *et al.*, 1998), (Utracki, 2002). For the polymer blend systems, such as PTT/mPE (Jafari *et al.*, 2005), PTT/PP (Xue *et al.*, 2007, Xue *et al.*, 2007, Wang *et al.*, 2009), PTT/PET (Run *et al.*, 2009), PTT/PS (Huang, 2003), PTT/acrylonitrile–butadiene–styrene (ABS) (Xue *et al.*, 2007), and etc., improve their impact strength, crystallization, or other mechanical and physical properties. Polyethylene (PE) is the most widely used plastic throughout the world. It has several types such as high-density polyethylene (HDPE), *low-density polyethylene* (LDPE) and linear low density polyethylene (LLDPE). PE is easy to process, insensitive to moisture, good flexibility, good impact resistance, and relatively inexpensive (Sinthavathavorn *et al.*, 2008). Therefore, the blending of PTT with PE can combine the desirable characteristics of both materials and can enhance their properties such as strength, low temperature impact resistance, and high temperature capability which these are all importance for automotive applications.

Theoretically, PTT and PE blends are thermodynamically immiscible and mechanically incompatible which show a separation tendency, and lead to a coarse structure and low interfacial adhesion and result in poor mechanical properties of the final material. So, the directly mixed PTT/PE cannot serve as any useful product. Immiscible blends can be improved by adding a third component, which is an interfacially active polymer or a compatibilizer. It can improve physical and/or

chemical interactions between each polymer (Koning *et al.*, 1998), (Utracki, 2002). In this research, maleic anhydride grafted high-density polyethylene (MAH–g–HDPE) or Fusabond and ethylene-methacrylic acid neutralized sodium metal (Na-EMAA) or Surlyn were selected as compatibilizers for PTT/PE blends since they are widely used and easily available.

The aim of the this work is to study compatibilization effect of MAH-g-HDPE and Na-EMAA on the blends of PTT and PE. Characterization of mechanical, rheological, and morphological properties of obtained polmer blends

4.3 Experimental

4.3.1 Materials

Poly(trimethylene terephthalate), Sorona® 3301 NC010 (density 1.32 g/cm^3) was supplied by DuPont (USA). High density polyethylene, InnoPlus® HD2208J (density 0.961 g/ cm^3) and Liner low density, InnoPlus® LL8420A (density 0.924 g/cm^3) were an injection molding grade which supplied by PTT Global Chemical Public Co.,Ltd. (Thailand). Maleic anhydride grafted high-density polyethylene (MAH–g–HDPE), Fusabond® E MB100D (density 0.960 g/cm^3) and ethylene-methacrylic acid neutralized sodium metal (Na-EMAA), Surlyn® 8940 (density 0.95 g/cm^3) were supplied by DuPont (USA).

4.3.2 Blend Preparation

Prior to melt mixing, all materials have dried in oven at 60°C for 24 h. Then, the materials with different ratios (Table 4.1) were placed into a tumble mixer to premix for 10 min. Then these materials were fed through a Collin D8017 T-20 twin-screw extruder by using a screw speed of 40 rpm and temperature profile follow Table 4.2. The blends were extruded through the strands die, those extrudates were cooled in a water bath, then dried at ambient temperature and were cut from a pneumatic die cutter.

4.3.3 Specimen Preparation

4.3.3.1 *Compression Molding*

DSC specimens were obtained by using a Lab-Tech compression machine. The pellets were placed in an aluminum frame mold and preheated at 250 °C for 10 min between the plates without any applied pressure to allow for complete melting. After this period, lading pressure of 40 kg/cm^2 to mould at the same temperature for 5 min. The sample was cooled naturally for 5 min under same pressure.

4.3.3.2 *Injection Molding*

Tensile, impact, and DMA test specimens were obtained by injection molding machine (Battenfeld BA 250 CDC) with 22 mm of diameter. The

temperature profile for forming specimen was 230, 245, 250, and 250 °C respectively except for pure HDPE and pure LLDPE using 160, 165, 170, and 175 °C. The screw speed was 20 rpm, and injection pressure was set as 75 bars.

4.3.4 Characterization

4.3.4.1 *Tensile Testing*

A Universal testing machine was used to measure the tensile strength, Young's modulus, and elongation at break of the blends. The tests were followed according to ASTM D638 test procedure, using a crosshead speed of 50 mm/min. Results were averaged from five specimens per each batch of the blends.

4.3.4.2 *Impact Testing*

Izod impact strength was measured using a Zwick impact tester according to ASTM D256 test procedure with a 2.7 J pendulum. Results were averaged from ten specimens per each batch of the blends.

4.3.4.3 *Differential Scanning Calorimetry (DSC)*

Thermal analysis was carried out on a differential scanning calorimeter, DSC Q1000. All scans were made under nitrogen atmosphere to minimize oxidative degradation. The temperature calibration of the DSC was obtained by measuring the melting temperature of indium as a standard. 10 mg of samples were encapsulated in an aluminum pan, heated from -85 °C to 275 °C at a heating rate of 10 °C/min, held for 1 min at this temperature to remove their thermal history, followed by cooling to -85 °C at 10 °C/min, and held for 5 min again. After that, samples reheat to 275 °C with heating rate of 10 °C/min. The crystallinity of the sample was also determined from a knowledge of the ratio of the melting enthalpy for 100% crystallinity of pure components. The absolute crystallinity of the blend was calculated using equation (1);

$$\chi_c = \frac{\Delta H \times 100\%}{\Delta H_f \times \text{wt.fraction}} \qquad (1)$$

where; χ_c is the % weight fractional crystallinity, ΔH is the melting enthalpy of the component present in the blends, ΔHf is the heat o fusion for the 100% crystallinity

of the pure component, (145 J/g for PTT, and 293 J/g for HDPE and LLDPE) (Piorkowska *et al.*, 2013).

4.3.4.4 *Rheometry*

All blends are measured for the shear viscosity by the capillary rheometer (CEAST Rheolgic 5000). The investigation is recorded at temperature 250°C with a temperature tolerance is set at ±0.5°C. The inner diameter of the barrel is 15 mm, while the inner diameter and the length of the die were 1 and 20 mm (i.e. L/D = 20), respectively. Approximately 50 ml pellets were inserted to the bore and pressed well. After preheating 300 seconds, an automatic data collection system is used to analyze the test results.

4.3.4.5 *Melt Flow Index Testing*

The weight of the polymer flow for 10 min was measured by a melt flow indexer under a 2.16-kg load at 250°C according to ASTM D1238 test procedure.

4.3.4.6 *Scanning Electron Microscopy (SEM)*

Fracture micrographs were studies using a scanning electron microscope (JEOL, JSM-S410LV), operated at 15 kV. The sample fractured under liquid nitrogen. The specimens were then coated with gold to make samples electrically conductive. The number average diameter (d_n) was calculated using equation (2);

$$d_n = \Sigma(n_i d_i)/\Sigma n_i \qquad (2)$$

where; n_i is the number of droplet and d_i is the diameter of the ith droplet.

4.4 Results and Discussion

4.4.1 PTT/HDPE Blends

4.4.1.1 *Phase Morphology*

The morphology of difference blends was investigated by scanning electron microscope (SEM) on freeze-fracture specimens. SEM micrographs of freeze-fracture surfaces of uncompatibilized blends showed two phases morphology with phase separation between PTT and HDPE phase as shown in Figure 4.1. The presence of dispersed phase, consisting of spherical droplets imbedded in a matrix, was observed from the micrographs over the whole composition range. It was obvious from Figure 4.1 that the adhesion between PTT and HDPE was very poor.

The micrographs of compatibilized PTT/HDPE blends with different amount of MAH-g-HDPE are shown in Figure 4.2 and 4.3. The addition of MAH-g-HDPE as compatibilizer resulted in a decrease of the dispersed phase size. The reduction of dispersed phase size was due to the ability of the compatibilizer to reduce the interfacial tension between the dispersed phase and the matrix phase. The reduction of the interfacial tension could be caused by the chemical reaction between the carbonyl groups of MAH-g-HDPE and hydroxyl groups of PTT increased the interfacial adhesion of the blend (Yang *et al.*, 2002, Qi *et al.*, 2006).

The phase morphology of the blends with different amount of Na-EMAA was also investigated as shown in Figure 4.4 and 4.5. The addition of ionomer showed a decreased of the dispersed phase size. The reduction of dispersed phase size when the compatibilizer was added was due to Na-EMAA to reduce the interfacial tension between two phases. These observations could be caused by the ethylene segments of Na-EMAA compatible to the HDPE and the Na-EMAA carboxylic acid reacted with the hydroxyl end groups of PTT (Retolaza *et al.*, 2002, Retolaza *et al.*, 2003).

Table 4.3 and 4.4 show the number average size of dispersed phase of the uncompilized and compatibilzied blends with MAH-g-HDPE and Na-EMAA, repectively. The number average size of dispersed phase ranged between 0.85 and 3.57 μm. The uncompatilized blends demonstrated the biggest diameter of

dispersed phase size. All compatibilized blends both with MAH-g-HDPE and Na-EMAA displayed much smaller diameter. The reduction of dispersed phase size when the compatibilizer was added was due to compatibilizer to reduce the interfacial tension between two phases. As show in Table 4.3 and 4.4, the types of compatiblizer did not effect on dispersed phase size of the blends.

4.4.1.2 *Mechanical Properties*

Table 4.5 shows the mechanical properties, tensile strength, Young's modulus, and impact strength, of PTT/HDPE blends with and without compatibilzer.

4.4.1.2.1 Tensile Properties

The results showed that the Young's modulus and the tensile strength of neat PTT were higher than neat HDPE (see in Table 4.5), which indicated that PTT gave the higher strength and stiffness than HDPE.

The tensile properties, the Young's modulus and the tensile strength of all uncompatibilized blends were lower than pure PTT. The tensile properties decrease with increasing HDPE. The adding of flexible polymer (HDPE) caused the reducing in the Young's modulus and tensile strength. The reduction of these properties also could be attributed to the poor interfacial adhesion between two phases which resulted in the weak stress transfer from one phase to another phase. Furthermore, the dispersed phase in the matrix also leaded to the presence of stress concentrations that give a weak point in the blends.

The effect of MAH-g-HDPE as a compatibilizer on tensile properties was investigated. As shown in Table 4.5, the Young's modulus and tensile strength of the compatibilzed blends were higher than uncompatbilized blends. The improvement of tensile properties due to the addition of MAH-g-HDPE brought about finer dispersed phase and stronger adhesion between PTT and HDPE phases (Yang *et al.*, 2002, Qi *et al.*, 2006).

The Young's modulus and tensile strength of PTT/HDPE were also enhanced by addition of Na-EMAA as shown in Table 4.5. This behavior was due to the chemical interaction between compatibilizer and PTT. This indicated that compatibilizer improved the interfacial adhesion and causes the

dispersed phase size to decrease resulting in better stress transfer between two phased were obtain.

When compare between 2 compatibilizers, MAH-g-HDPE blends gave the higher tensile strength than Na-EMAA (except PTT/HDPE 80/20). For the Young's modulus, MAH-g-HDPE blends also gave higher value than Na-EMAA (except PTT/HDPE 60/40).

4.4.1.2.2 Impact Properties

The results show that neat HDPE gave the higher impact strength than neat PTT (see in Table 4.5) due to HDPE had more flexible main chain than PTT, when it was impacted, it could absorb the energy, then dissipate and transfer the energy which lead HDPE shown better impact properties.

The impact strength of uncompatiblized blends increased as HDPE content increased. This could be due to the incorporation of HDPE, which has more flexible chain, and then it showed better impact properties.

The effect of MAH-g-HDPE contents on the impact strength was also shown in Table 4.5. The results showed that the impact strength of compatbilized blends were higher than uncompatiblized blends. The improvement in compatibility of polymers blends would due to smaller dispersed phase sizes and high interfacial adhesion. There was interaction between carboxylate groups of the MAH-g-HDPE and hydroxyl groups of PTT. Therefore, compatibilized blends should be much better than uncompatbilized blends, which resulted in the enhancement of impact resistance or toughness (Yang *et al.*, 2002, Qi *et al.*, 2006). However, the reaction rate, of carbonyl groups and hydroxyl groups, for forming an ester was very low (Sun *et al.*, 1996), which may be one of reasons that impact strength of the blends was not dramatically improved.

The effect of Na-EMAA contents on the impact strength was also investigated. The results showed that the compatbilized blends gave higher than uncompatiblized blends (see in Table 4.5). This improvement can also be explained by the improved adhesion between the phases, which allow absorbed energy to transfer form on phase to another phase (Guerrero *et al.*, 2001, Retolaza *et al.*, 2002).

When compare between 2 compatibilizers, PTT/HDPE blends with Na-EMAA gave the higher impact strength than PTT/HDPE blends with MAH-g-HDPE.

4.4.1.3 *Rheological Behavior*

The plots of viscosity versus shear rate for the neat polymers were measured at temperature 250°C and at shear rate range from 50 to 6400 s^{-1}, which are shown in Figure 4.6. The results showed that neat PTT showed relatively lower viscosity than neat HDPE.

All uncompatibilized blends exhibit shear thinning behavior which interpreted as the viscosity decreased with increasing shear rate (see in Figure 4.7) due to the induced chain orientation, resulting in a lower entanglement density. The shear viscosity of the blends was found to decrease with decreasing HDPE.

The flow curves of compatibilized blends with difference amount of MAH-g-HDPE were shown in Figure 4.8. The results showed that shear viscosity of PTT/HDPE blends with MAH-g-HDPE increased with increasing of MAH-g-HDPE which may be related to the formation of covalent bonds between hydroxyl group of PTT and carboxylic acids in MAH-g-HDPE (Kang *et al.*, 1999, Charoenpongpool *et al.*, 2013).

The shear viscosity of compatibilized blends with difference amount of Na-EMAA is shown in Figure 4.9. Using Na-EMAA to compatibilized the blends can enhance the viscosity. As ionomer was added, a more homogeneous dispersion of one phase into another was obtained, indicating more interactions at the interface between the two polymers and hence less slippage at the interface in the presence of ionomer. This may be the reason for higher viscosities of the blends on addition of Na-EMAA (Joshi *et al.*, 1992).

4.4.1.4 *Melt Flow Index*

The melt flow index of neat polymers was investigated. The results showed that PTT gave the higher melt flow index than HDPE which indicated that PTT gave the lower viscosity or the easier flow than HDPE.

The compatibilizers addition usually increases the melt viscosity of immiscible blends because it increases the interaction between components. Figure 4.10 shows the effect of compatibilizers on the melt flow index of PTT/HDPE blends. The results show that melt flow index of the blends decreased with increasing MAH-g-HDPE contents. The decrease of the melt flow index or the increase of the viscosity may be related to the expected reaction and the increased interfacial interaction of the PTT/HDPE/HDPE-g-MAH blending system (Kang et al., 1999).

The effect of Na-EMAA contents on the melt flow index of the blends was also shown in Figure 4.10. The results show that melt flow index of the blends decreased with increasing Na-EMAA contents. The decrease of the melt flow index or the increase of the viscosity could be related to the expected reaction and Na-EMAA can increase the interfacial adhesion between two phases. This could be the reason for lower melt flow index of the blends on addition of Na-EMAA (Joshi et al., 1992).

At 5 phr of compatibilizer, Na-EMAA blends exhibited higher melt flow index than MAH-g-HDPE.

4.4.1.5 *DSC Analysis*

Effect of compatiblization on the melting and crystallization temperatures and weight fraction crystallinity of each component of the blend were studies.

As the results, the crystallization temperature (T_c) peak of neat PTT and neat HDPE occurred at 180.0°C and 118.7°C, respectively.

Figure 4.11 shows DSC exothermic thermograms of uncompatibilized PTT/HDPE. The results showed that there were no changes in T_c of the HDPE component in the PTT/HDPE. On the other hand, T_c of PTT component was relatively lower than T_c of pure PTT. It is possible that HDPE retarded PTT

crystallization which the results showed that T_c of PTT in the uncompatiblized blends decrease with increasing HDPE contents.

DSC exothermic thermograms of PTT/HDPE with difference amount of MAH-g-HDPE are shown in Figure 4.12. The results show that the addition of MAH-g-HDPE shifted the T_c of PTT phase to lower temperature but shifted T_c of HDPE phase to higher temperature. It indicated that the presence of MAH-g-HDPE retarded the crystallization of PTT but induced the crystallization of HDPE.

Figure 4.13 shows DSC exothermic thermograms of PTT/HDPE with difference amount of Na-EMAA. The results show that the addition of Na-EMAA shifted the T_c of PTT phase to higher temperature but shifted T_c of HDPE phase to lower temperature. This indicated the nucleation effect of Na-EMAA on the crystallization of PTT.

As the results, the melting temperature (T_m) of neat PTT and HDPE was 227.7 °C and 132.4 °C, respectively.

Figure 4.14 shows DSC melting thermograms of PTT/HDPE blends without compatibilizer. The T_m peaks of PTT in PTT/HDPE blends were not difference from pure PTT. On the other hand, the T_m peaks of HDPE in the blends were lower than that pure HDPE. This indicated that, in the presence of PTT, the crystalline phase was less perfect.

DSC melting thermograms of PTT/HDPE with difference amount of MAH-g-HDPE are shown in Figure 4.15. The results show that the addition of MAH-g-HDPE did not affect both the T_m of PTT phase and the T_m of HDPE phase.

As shown in Figure 4.16, the results show that melting temperature peaks of each component in the PTT/HDPE blends with Na-EMAA were not difference from uncompatilized blends which the addition of Na-EMAA still gave lower T_m peaks of HDPE components when compared with pure HDPE and did not affect to PTT's T_m peaks.

The weight fraction crystallinity (χ_c) of the blend and neat components is shown in Table 4.6. It can be observed from the table that all

composition ratios of uncompatibilized blends showed that the weight fraction crystallinity for both PTT and HDPE components was less than pure polymers. This implied that the crystallization of one component was affected by addition of another component. By adding MAH-g-HDPE or Na-EMAA in PTT/HDPE blends, the χ_c of both PTT and HDPE decreased.

4.4.2 PTT/LLDPE Blends

4.4.2.1 *Phase Morphology*

SEM micrographs of freeze-fracture surfaces of uncompatibilized PTT/LLDPE blends are shown in Figure 4.17. The results show that there were two phases morphology with phase separation between PTT and LLDPE phase. The presence of dispersed phase, consisting of spherical droplets imbedded in a matrix, was observed from the micrographs over the whole composition range. It was obvious from Figure 4.17 that the adhesion between PTT and LLDPE was very poor.

The micrographs of compatibilized PTT/LLDPE and PTT/LLDPE blends with different amount of MAH-g-HDPE are shown in Figure 4.18 and 4.19. The presence of MAH-g-HDPE resulted in a decrease of the dispersed phase size. The reduction of dispersed phase size was due to MAH-g-HDPE can reduce the interfacial tension between the dispersed phase and the matrix phase which caused by the chemical reaction between the carbonyl groups of MAH-g-HDPE and hydroxyl groups of PTT increased the interfacial adhesion of the blend (Yang *et al.*, 2002, Qi *et al.*, 2006).

Figure 4.20 and 4.21 show the phase morphology of the blends with different amount of Na-EMAA. The addition of ionomer showed a decreased of the dispersed phase size. The reduction of dispersed phase size when the compatibilizer was added was due to Na-EMAA can reduce the interfacial tension between two phases which could be caused by the ethylene segments of Na-EMAA compatible to the HDPE and the Na-EMAA carboxylic acid reacted with the hydroxyl end groups of PTT (Retolaza *et al.*, 2002, Retolaza *et al.*, 2003).

The effect of compatibilizer on the number average size of dispersed phase of the uncompilized and compatibilzied blends is shown in Table

4.7 and 4.8. The results show that the number average size of dispersed phase ranged between 1.20 and 3.43 μm. The uncompatilized blends showed the biggest diameter of dispersed phase size. All compatibilized blends both with MAH-g-HDPE and Na-EMAA exhibited smaller diameter of dispersed phase. The reduction of dispersed phase size was due to compatibilizer to reduce the interfacial tension between two phases. As show in Table 4.7 and 4.8, the types of compatiblizer did not effect on dispensed phase size of the blends which show the same effect with PTT/HDPE blends.

4.4.2.2 *Mechanical Properties*

The mechanical properties including tensile strength, Young's modulus, and impact strength of PTT/HDPE blends with and without compatibilzer are shown in Table 4.9.

4.4.2.2.1 Tensile Properties

The results showed that the Young's modulus and the tensile strength of neat PTT were higher than neat LLDPE (see in Table 4.9), which indicated that PTT gave the higher strength and stiffness than LLDPE.

The tensile properties, the Young's modulus and the tensile strength of all uncompatibilized blends were lower than pure PTT. The tensile properties decrease with increasing LLDPE because LLDPE was the flexible chain which gave relatively low strength and stiffness. The reduction of these properties also could be attributed to the poor interfacial adhesion between two phases which resulted in the weak stress transfer from one phase to another phase. Furthermore, the dispersed phase in the matrix also leaded to the presence of stress concentrations that give a weak point in the blends.

The effect of MAH-g-HDPE as a compatibilizer on tensile properties is shown in Table 4.9. As results, the Young's modulus and tensile strength of the compatibilzed PTT/LLDPE blends were higher than uncompatbilized blends. The reason of improvement of tensile properties was the same with PTT/HDPE/MAH-g-HDPE blends that had discussed in PTT/HDPE blends part that the improvement of tensile properties due to the addition of MAH-g-HDPE brought about finer dispersed phase and stronger adhesion between PTT and LLDPE phases (Yang *et al.*, 2002, Qi *et al.*, 2006).

The Young's modulus and tensile strength of PTT/LLDPE were also enhanced by addition of Na-EMAA as shown in Table 4.9. The reason of improvement of tensile properties was the same with PTT/HDPE/Na-EMAA blends that had discussed in PTT/HDPE blends part which this behavior was due to the chemical interaction between compatibilizer and PTT. This indicated that compatibilizer improved the interfacial adhesion and causes the dispersed phase size to decrease resulting in better stress transfer between two phased were obtain.

When compare between 2 compatibilizers, MAH-g-HDPE blends gave the higher tensile strength and Young's modulus than Na-EMAA (except Young's modulus of PTT/LLDPE: 80/20 with 0.1 and 0.5 phr of compatibilizer and Tensile strength and Young's modulus of PTT/LLDPE: 60/40 with 0.1 phr of compatibilizer).

When compare between PTT/HDPE and PTT/LLDPE blends, PTT/LLDPE blends show lower tensile strength and Young's modulus than PTT/HDPE blends.

4.4.2.2.2 Impact Properties

The results show that neat LLDPE gave the higher impact strength than neat PTT (see in Table 4.9) due to LLDPE had short branch chains so the chains were flexible, when it was impacted, it could absorb the energy, then dissipate and transfer the energy which lead LLDPE shown good impact properties.

The impact strength of uncompatiblized blends increased as LLDPE content increased. This could be due to the incorporation of LLDPE, which has more flexible chain, and then it showed better impact properties.

The effect of MAH-g-HDPE contents on the impact strength was also shown in Table 4.9. The results showed that the impact strength of compatbilized blends were higher than uncompatiblized blends. The reason of improvement of impact properties was the same with PTT/HDPE/MAH-g-HDPE blends that had discussed in PTT/HDPE blends part that the improvement in compatibility of polymers blends would due to smaller dispersed phase sizes and high interfacial adhesion. There was interaction between carboxylate groups of the MAH-g-HDPE and hydroxyl groups of PTT. Therefore, compatibilized blends

should be much better than uncompatbilized blends, which resulted in the enhancement of impact resistance or toughness (Yang *et al.*, 2002, Qi *et al.*, 2006).

The effect of Na-EMAA contents on the impact strength of PTT/LLDPE blends was also investigated. The results showed that the compatbilized blends gave higher than uncompatiblized blends (see in Table 4.5). This improvement can also be explained by the improved adhesion between the phases, which allow absorbed energy to transfer form on phase to another phase (Guerrero *et al.*, 2001, Retolaza *et al.*, 2002).

When compare between 2 compatibilizers, PTT/LLDPE showed the difference effect with PTT/HDPE blends that the type of compatibilizer did not effect on impact properties of the blends.

4.4.2.3 *Rheological Behavior*

The plots of viscosity versus shear rate for the neat polymers were measured at temperature 250°C and at shear rate range from 50 to 6400 s^{-1}, which are shown in Figure 4.22. The results showed that neat LLDPE showed relatively lower viscosity than neat PTT.

All uncompatibilized blends showed shear thinning behavior which interpreted as the viscosity decreased with increasing shear rate (see in Figure 4.23) due to the induced chain orientation, resulting in a lower entanglement density. The shear viscosity of the blends was found to decrease with increasing LLDPE.

The flow curves of compatibilized blends with difference amount of MAH-g-HDPE were shown in Figure 4.24. The results showed that shear viscosity of PTT/LLDPE blends increased when MAH-g-HDPE was added which may be related to the formation of covalent bonds between hydroxyl group of PTT and carboxylic acids in MAH-g-HDPE (Kang *et al.*, 1999, Charoenpongpool *et al.*, 2013).

The shear viscosity of compatibilized blends with difference amount of Na-EMAA is shown in Figure 4.25. Using Na-EMAA as compatibilizer can enhance the viscosity. As ionomer was added, a more homogeneous dispersion of one phase into another was obtained, indicating more interactions at the interface between the two polymers and hence less slippage at the interface in the presence of

ionomer. This may be the reason for higher viscosities of the blends on addition of Na-EMAA (Joshi *et al.*, 1992).

4.4.2.4 *Melt Flow Index*

The melt flow index of neat polymers was also studied. The results showed that LLDPE gave the higher melt flow index than PTT which indicated that LLDPE gave the lower viscosity or the easier flow than PTT.

Figure 4.26 shows the effect of compatibilizers on the melt flow index of PTT/LLDPE blends. The results show that melt flow index of the blends decreased with increasing MAH-g-HDPE contents. The decrease of the melt flow index or the increase of the viscosity may be related to the expected reaction and the increased interfacial interaction of the PTT/LLDPE/HDPE-g-MAH blending system (Kang et al., 1999).

The effect of Na-EMAA contents on the melt flow index of the blends was also shown in Figure 4.6. The results show that melt flow index of the blends decreased with increasing Na-EMAA contents. The decrease of the melt flow index or the increase of the viscosity could be related to the expected reaction and Na-EMAA can increase the interfacial adhesion between two phases. This could be the reason for lower melt flow index of the blends on addition of Na-EMAA (Joshi et al., 1992).

At 5 phr of compatibilizer, Na-EMAA blends exhibited higher melt flow index than MAH-g-HDPE which also found in PTT/HDPE blends.

4.4.2.5 *DSC Analysis*

Effect of compatiblization on the melting and crystallization temperatures and weight fraction crystallinity of each component of the blend were studies.

As the results, the crystallization temperature (T_c) peak of neat PTT and neat LLDPE occurred at 180.0 °C and 110.5 °C, respectively.

Figure 4.27 and 4.28 show DSC exothermic thermograms of uncompatibilized PTT/HDPE. The results showed that there were no changes in T_c of the HDPE component in the PTT/HDPE. On the other hand, T_c of PTT component was relatively lower than T_c of pure PTT. It is possible that HDPE retarded PTT

crystallization which the results showed that T_c of PTT in the uncompatiblized blends decrease with increasing HDPE and LLDPE contents.

DSC exothermic thermograms of PTT/LLDPE with difference amount of MAH-g-HDPE are shown in Figure 4.28. The results show similar to PTT/HDPE/MAH-g-HDPE blends. The addition of MAH-g-HDPE shifted the T_c of PTT phase to lower temperature but shifted T_c of LLDPE phase to higher temperature. It indicated that the presence of MAH-g-HDPE retarded the crystallization of PTT but induced the crystallization of LLDPE.

Figure 4.29 shows DSC exothermic thermograms of PTT/LLDPE with difference amount of Na-EMAA. The results show that the addition of Na-EMAA shifted the T_c of PTT phase to higher temperature but shifted T_c of LLDPE phase to lower temperature. This indicated the nucleation effect of Na-EMAA on the crystallization of PTT which this effect also occurred in PTT/HDPE/Na-EMAA that already discuss in preview part.

As the result, the melting temperature (T_m) of neat PTT and LLDPE was 227.7 °C and 122.1 °C, respectively.

Figure 4.30 shows DSC melting thermograms of PTT/LLDPE blends without compatibilizer. The T_m peaks of PTT in PTT/LLDPE blends were not difference from pure PTT. On the other hand, the T_m peaks of LLDPE in the blends were higher than that neat LLDPE. This indicated that, in the presence of PTT, the crystalline phase was more perfect.

DSC melting thermograms of PTT/LLDPE with difference amount of MAH-g-HDPE are shown in Figure 4.31. The results were similar to PTT/HDPE blend that the addition of MAH-g-HDPE did not affect both the T_m of PTT phase and LLDPE phase.

As show in Figure 4.32, the results show similar to PTT/HDPE blend that melting temperature peaks of each component in the PTT/LLDPE blends with Na-EMAA were not difference from uncompatilized blends which the addition of Na-EMAA still gave lower T_m peaks of LLDPE components when compared with pure LLDPE and did not affect to PTT's T_m peaks.

The weight fraction crystallinity (χ_c) of the blend and neat components is shown in Table 4.10. It can be observed from the table that all composition ratios of uncompatibilized blends showed that the weight fraction crystallinity for both PTT and LLDPE components was less than pure polymers. This implied that the crystallization of one component was affected by addition of another component. By adding MAH-g-HDPE or Na-EMAA in PTT/LLDPE blends, the χ_c of both PTT and LLDPE decreased which similar to PTT/HDPE blends.

4.5 Conclusions

In this work, MAH-g-HDPE and Na-EMAA as compatibilizers were added to the PTT/HDPE and PTT/LLDPE blends by melt mixing. SEM micrographs show that the average size of the dispersed phase decreased by the addition of small amount of compatibilizer. Only 0.1 – 1 phr of compatibilizer was sufficient to produce maximum reduction in dispersed phase size. The mechanical properties increased with the addition of compatibilizer, including tensile strength, Young's modulus and impact strength. PTT/HPDE/Na-EMAA: 80/20/1 gave the highest tensile strength at 46.87 MPa while PTT/HDPE/MAH-g-HDPE : 80/20/1 gave the highest Young's modulus at 925 MPa and PTT/LLDPE/MAH-g-HDPE:60/40/1 gave the highest impact strength at 8.2 KJ/m^2.Viscosity of blends increased with increasing amount of compatibilizer and at 5 phr of compatibilizer, Na-EMAA blends gave higher melt flow index than MAH-g-HDPE blends. The addition of MAH-g-HDPE in the blends shifted T_c of PTT to lower temperature but shifted T_c of HDPE or LLDPE to higher temperature. On the other hand the addition of Na-EMAA shifted the T_c of PTT to higher temperature but shifted T_c of HDPE or LLDPE to lower temperature. The addition of MAH-g-HDPE and Na-EMAA did not effect to T_m of both PTT and HDPE or LLDPE. All composition ratios of uncompatibilized and compatbilized blends showed that % Crystallinity for both PTT and HDPE or LLDPE components was less than neat polymers.

4.6 Acknowledements

This thesis work is funded by the Petroleum and Petrochemical College; and the National Center of Excellence for Petroleum, Petrochemicals, and Advanced Materials, Thailand.

4.7 References

1. Charoenpongpool, S., Nithitanakul, M. and Grady, B.P. (2013). Melt-neutralization of maleic anhydride grafted on high-density polyethylene compatibilizer for polyamide-6/high-density polyethylene blend: effect of neutralization level on compatibility of the blend. Polymer Bulletin 70(1), 293-309.
2. Guerrero, C., Lozano, T., González, V. and Arroyo, E. (2001). Properties and morphology of poly (ethylene terephthalate) and high-density polyethylene blends. Journal of Applied Polymer Science 82(6), 1382-1390.
3. Huang, J.M. (2003). Polymer blends of poly (trimethylene terephthalate) and polystyrene compatibilized by styrene-glycidyl methacrylate copolymers. Journal of Applied Polymer Science 88(9), 2247-2252.
4. Jafari, S.H., Asadinezhad, A., Yavari, A., Khonakdar, H.A. and Böhme, F. (2005). Compatibilizing Effects on the Phase Morphology and Thermal Properties of Polymer Blends Based on PTT and m-LLDPE. Polymer Bulletin 54, 417–426.
5. Joshi, M., Misra, A. and Maiti, S.N. (1992). Poly(butylene terephthalate)/high density polyethylene alloys. II. Mechanical properties and rheology. Journal of Applied Polymer Science 45, 1837–1847.
6. Kang, T.K., Kim, Y., Lee, W.K., Park, H.D., Cho, W.J. and Ha, C.S. (1999). Properties of uncompatibilized and compatibilized poly (butylene terephthalate)–LLDPE blends. Journal of Applied Polymer Science 72(8), 989-997.
7. Koning, C., Duin, M.V., Pagnoulle, C. and Jerome, R. (1998). Strategies For Compatibilization Of Polymer Blends. Prog. Polym. Sci. 23, 707-757.
8. Piorkowska, E. and Rutledge, G.C. (2013). Handbook of Polymer Crystallization: Wiley.
9. Qi, R., Nie, J., Zhou, C., Mao, D. and Zhang, B. (2006). Influence of High Density Polyethylene-g-Maleic Anhydride on Compatibility and Properties of Poly(butylene terephthalate)/High Density Polyethylene Blends. Journal of Applied Polymer Science 12, 6081–6087.
10. Retolaza, A., Eguiazabal, J. and Nazabal, J. (2002). A lithium ionomer of poly (ethylene-co-methacrylic acid) copolymer as compatibilizer for blends of poly (ethylene terephthalate) and high density polyethylene. Polymer Engineering & Science 42(11), 2072-2083.

11. Retolaza, A., Eguiazabal, J. and Nazabal, J. (2003). Poly (ethylene-co-methacrylic acid)–lithium ionomer as a compatibilizer for poly (ethylene terephthalate)/linear low-density polyethylene blends. Journal of Applied Polymer Science 87(8), 1322-1328.
12. Rex, W.J. and Tennant, D.J. (1949). Polymeric linear terephthalic esters, Google Patents.
13. Run, M.-t., Wang, H.-s. and Li, X. (2012). Morphology, mechanical, rheological, and thermal properties study on the PTT/ABS/SCF composites. Composite Interfaces 19(5), 333-351.
14. Run, M., Hao, Y. and Yao, C. (2009). Melt-crystallization behavior and isothermal crystallization kinetics of crystalline/crystalline blends of poly (ethylene terephthalate)/poly (trimethylene terephthalate). Thermochimica Acta 495(1), 51-56.
15. Sinthavathavorn, W., Nithitanakul, M., Magaraphan, R. and Grady, B.P. (2008). Blends of Polyamide 6 with Low-Density Polyethylene Compatibilized with Ethylene–Methacrylic Acid Based Copolymer Ionomers: Effect of Neutralizing Cations. Journal of Applied Polymer Science 107, 3090–3098.
16. Sun, Y.-J., Hu, G.-H., Lambla, M. and Kotlar, H.K. (1996). In situ compatibilization of polypropylene and poly (butylene terephthalate) polymer blends by one-step reactive extrusion. Polymer 37(18), 4119-4127.
17. Utracki, L.A. (2002). Compatibilization of Polymer Blends. Can. J. Chem. Eng. 80, 1008–1016.
18. Wang, Y. and Run, M. (2009). Non-isothermal crystallization kinetic and compatibility of PTT/PP blends by using maleic anhydride grafted polypropylene as compatibilizer. J Polym Res 16, 725–737.
19. Xue, M.L., Yu, Y.L. and Chuah, H.H. (2007). Reactive Compatibilization of Poly(trimethylene terephthalate)/Polypropylene Blends by Polypropylene-graft-Maleic Anhydride. Part 2. Crystallization Behavior. Journal of Macromolecular Science 46, 603–615.
20. Xue, M.L., Yu, Y.L., Chuah, H.H. and Qiu, G.X. (2007). Reactive Compatibilization of Poly(trimethylene terephthalate)/Polypropylene Blends byPolypropylene-graft-Maleic Anhydride. Part 1. Rheology, Morphology, Melting, and Mechanical Properties. Journal of Macromolecular Science 46, 387–401.
21. Xue, M.L., Yu, Y.L., Chuah, H.H., Rhee, J.M., Kim, N.H. and Lee, J.H. (2007). Miscibility and compatibilization of poly(trimethylene terephthalate)/acrylonitrile–butadiene–styrene blends. European Polymer Journal 43, 3826–3837.
22. Yang, J., Shi, D., Yao, Z., Xin, Z. and Yin, J. (2002). Effect of the Compatibilization of Linear Low-Density Polyethylene-g-Acrylic Acid on the Morphology and Mechanical Properties of Poly(butylene terephthalate)/Linear Low-Density Polyethylene Blends. Journal of Applied Polymer Science 84, 1059–1066.

Table 4.1 Blend compositions

	Concentration (%wt)			
	PPT	HDPE	LLDPE	Compatibilizer
PTT	100	-	-	-
HDPE	-	100	-	-
LLDPE	-	-	100	-
PTT/HDPE/MAH-g-HDPE	80	20	-	0, 0.1, 0.5, 1, 5 phr
	60	40	-	0, 0.1, 0.5, 1, 5phr
PTT/HDPE/Na-EMAA	80	20	-	0, 0.1, 0.5, 1, 5phr
	60	40	-	0, 0.1, 0.5, 1, 5phr
PTT/LLDPE/MAH-g-HDPE	80	-	20	0, 0.1, 0.5, 1, 5phr
	60	-	40	0, 0.1, 0.5, 1, 5phr
PTT/LLDPE/Na-EMAA	80	-	20	0, 0.1, 0.5, 1, 5phr
	60	-	40	0, 0.1, 0.5, 1, 5phr

Table 4.2 Temperature profile of twin screw extruder

Extruder Zone	1	2	3	4	5	6	7	8
Temperature (°C)	120	240	245	245	250	250	250	250

Table 4.3 Dispersed phased size of PTT/HDPE/MAH-g-HDPE blends

MAH-g-HDPE content (phr)	PTT/HDPE ratio	
	80/20	60/40
0	2.99	3.57
0.1	1.07	2.57
0.5	1.79	1.17
1	2.27	1.22
5	2.06	1.07

Table 4.4 Dispersed phased size of PTT/HDPE/Na-EMAA blends

Na-EMAA content (phr)	PTT/HDPE ratio	
	80/20	60/40
0	2.99	3.57
0.1	1.84	0.85
0.5	2.63	1.42
1	1.61	1.37
5	0.86	1.26

Table 4.5 Mechanical properties of PTT/HDPE blends with and without compatibilizer

System	Ratio	Tensile strength (MPa)		Young's modulus (MPa)		Impact strength (KJ/m^2)	
		Average	SD	Average	SD	Average	SD
PTT	100	60.26	0.20	1056.72	17.48	7.0	0.3
PTT/HDPE	80/20	44.45	0.49	902.92	25.70	6.9	0.0
PTT/HDPE/MAH-g-HDPE	80/20/0.1	44.56	0.49	914.70	44.49	7.2	0.4
PTT/HDPE/MAH-g-HDPE	80/20/0.5	44.71	0.40	899.94	42.76	7.3	0.3
PTT/HDPE/MAH-g-HDPE	80/20/1	45.96	0.31	925.44	27.06	7.3	0.2
PTT/HDPE/MAH-g-HDPE	80/20/5	43.42	0.51	875.80	37.76	7.3	0.2
PTT/HDPE/Na-EMAA	80/20/0.1	46.58	0.76	898.79	30.53	7.5	0.1
PTT/HDPE/Na-EMAA	80/20/0.5	46.27	0.60	898.71	31.75	7.5	0.1
PTT/HDPE/Na-EMAA	80/20/1	46.87	0.24	916.86	48.53	7.5	0.1
PTT/HDPE/Na-EMAA	80/20/5	42.73	0.49	819.13	42.70	7.5	0.1
PTT/HDPE	60/40	39.14	0.62	795.34	16.47	7.8	0.5
PTT/HDPE/MAH-g-HDPE	60/40/0.1	39.83	0.87	802.00	53.83	7.8	0.2
PTT/HDPE/MAH-g-HDPE	60/40/0.5	40.54	0.38	817.09	51.87	8.0	0.2
PTT/HDPE/MAH-g-HDPE	60/40/1	40.36	0.51	819.01	21.38	7.8	0.3
PTT/HDPE/MAH-g-HDPE	60/40/5	39.43	0.38	760.88	41.44	7.8	0.3
PTT/HDPE/Na-EMAA	60/40/0.1	40.68	3.20	829.71	25.50	7.9	0.5
PTT/HDPE/Na-EMAA	60/40/0.5	39.53	2.89	824.40	22.14	8.2	0.3
PTT/HDPE/Na-EMAA	60/40/1	39.38	3.56	812.94	47.75	7.9	0.2
PTT/HDPE/Na-EMAA	60/40/5	37.95	0.75	783.71	29.64	7.9	0.3
HDPE	100	24.47	0.52	613.25	26.19	11.9	0.5

Table 4.6 Weight fraction crystallinity of PTT/HDPE with and without compatibilizer

Systems	ratio	$\%\chi_c$ of HDPE	$\%\chi_c$ of PTT
PTT	100	-	33.1
HDPE	100	71.3	-
PTT/HDPE	80/20	66.6	29.8
PTT/HDPE/MAH-g-HDPE	80/20/0.1	59.1	30.5
PTT/HDPE/MAH-g-HDPE	80/20/0.5	64.7	30.8
PTT/HDPE/MAH-g-HDPE	80/20/1	61.9	30.5
PTT/HDPE/MAH-g-HDPE	80/20/5	66.6	30.3
PTT/HDPE/Na-EMAA	80/20/0.1	58.4	31.8
PTT/HDPE/Na-EMAA	80/20/0.5	61.4	30.9
PTT/HDPE/Na-EMAA	80/20/1	59.3	32.3
PTT/HDPE/Na-EMAA	80/20/5	55.9	32.5
PTT/HDPE	60/40	69.4	28.4
PTT/HDPE/MAH-g-HDPE	60/40/0.1	65	30
PTT/HDPE/MAH-g-HDPE	60/40/0.5	61.6	29.2
PTT/HDPE/MAH-g-HDPE	60/40/1	64.5	29.9
PTT/HDPE/MAH-g-HDPE	60/40/5	68.3	29.2
PTT/HDPE/Na-EMAA	60/40/0.1	63.8	29.4
PTT/HDPE/Na-EMAA	60/40/0.5	67.2	28.5
PTT/HDPE/Na-EMAA	60/40/1	63.5	30.1
PTT/HDPE/Na-EMAA	60/40/5	59.9	27.2

Table 4.7 Dispersed phased size of PTT/HDPE/MAH-g-HDPE blends

MAH-g-HDPE content (phr)	PTT/LLDPE ratio	
	80/20	60/40
0	2.13 μm	3.43 μm
0.1	1.73 μm	1.62 μm
0.5	1.36 μm	2.18 μm
1	1.77 μm	1.29 μm
5	1.31 μm	1.66 μm

Table 4.8 Dispersed phased size of PTT/HDPE/Na-EMAA blends

Na-EMAA content (phr)	PTT/LLDPE ratio	
	80/20	60/40
0	2.13 μm	3.43 μm
0.1	1.80 μm	1.20 μm
0.5	1.76 μm	2.10 μm
1	1.27 μm	1.77 μm
5	1.59 μm	1.82 μm

Table 4.9 Mechanical properties of PTT/HDPE blends with and without compatibilizer

System	Ratio	Tensile strength (MPa)		Young's modulus (MPa)		Impact strength (KJ/m^2)	
		Average	SD	Average	SD	Average	SD
PTT	100	60.26	0.20	1056.72	17.48	7.0	0.3
PTT/LLDPE	80/20	39.70	1.05	710.76	33.46	7.4	0.6
PTT/LLDPE/MAH-g-HDPE	80/20/0.1	41.66	0.11	748.08	20.11	7.9	0.4
PTT/LLDPE /MAH-g-HDPE	80/20/0.5	42.39	0.54	763.72	16.89	7.9	0.4
PTT/LLDPE/MAH-g-HDPE	80/20/1	41.42	0.50	794.74	8.42	7.6	0.5
PTT/LLDPE /MAH-g-HDPE	80/20/5	41.53	0.35	775.32	24.46	7.6	0.5
PTT/LLDPE /Na-EMAA	80/20/0.1	40.13	0.78	771.65	29.36	7.7	0.8
PTT/LLDPE /Na-EMAA	80/20/0.5	41.56	0.54	800.94	23.17	7.9	0.8
PTT/LLDPE /Na-EMAA	80/20/1	41.62	0.25	780.65	21.31	7.8	0.6
PTT/LLDPE /Na-EMAA	80/20/5	39.83	0.13	756.04	23.73	7.8	0.6
PTT/LLDPE	60/40	27.13	0.42	548.56	11.82	7.6	0.5
PTT/LLDPE/MAH-g-HDPE	60/40/0.1	26.95	0.34	557.45	15.68	8.1	0.6
PTT/LLDPE /MAH-g-HDPE	60/40/0.5	27.75	0.78	561.62	16.49	8.0	0.5
PTT/LLDPE/MAH-g-HDPE	60/40/1	27.86	0.71	555.41	8.33	8.2	0.5
PTT/LLDPE /MAH-g-HDPE	60/40/5	27.87	0.40	569.20	8.82	7.9	0.5
PTT/LLDPE /Na-EMAA	60/40/0.1	30.52	1.35	625.25	21.21	8.0	0.6
PTT/LLDPE /Na-EMAA	60/40/0.5	27.08	1.17	538.48	16.89	8.0	0.7
PTT/LLDPE /Na-EMAA	60/40/1	26.67	0.35	529.79	15.85	7.9	0.3
PTT/LLDPE /Na-EMAA	60/40/5	25.03	0.56	502.82	20.96	7.9	0.5
LLDPE	100	11.18	0.39	177.14	16.33	47.6	2.9

Table 4.10 Weight fraction crystallinity of PTT/HDPE with and without compatibilizer

Systems	ratio	$\%\chi_c$ of HDPE	$\%\chi_c$ of PTT
PTT	100	-	33.1
LLDPE	100	33.6	-
PTT/LLDPE	80/20	33.3	29.7
PTT/LLDPE/MAH-g-HDPE	80/20/0.1	27.0	31.0
PTT/LLDPE/MAH-g-HDPE	80/20/0.5	28.7	31.9
PTT/LLDPE/MAH-g-HDPE	80/20/1	31.1	30.6
PTT/LLDPE/MAH-g-HDPE	80/20/5	40.2	30.3
PTT/LLDPE/Na-EMAA	80/20/0.1	27.7	31.7
PTT/LLDPE/Na-EMAA	80/20/0.5	25.8	31.5
PTT/LLDPE/Na-EMAA	80/20/1	23.6	32.1
PTT/LLDPE/Na-EMAA	80/20/5	26.7	31.0
PTT/LLDPE	60/40	33.3	27.7
PTT/LLDPE/MAH-g-HDPE	60/40/0.1	31.3	29.2
PTT/LLDPE/MAH-g-HDPE	60/40/0.5	31.6	29.9
PTT/LLDPE/MAH-g-HDPE	60/40/1	31.3	28.8
PTT/LLDPE/MAH-g-HDPE	60/40/5	31.6	27.7
PTT/LLDPE/Na-EMAA	60/40/0.1	33.1	30.0
PTT/LLDPE/Na-EMAA	60/40/0.5	30.7	30.3
PTT/LLDPE/Na-EMAA	60/40/1	28.2	31.6
PTT/LLDPE/Na-EMAA	60/40/5	27.0	29.4

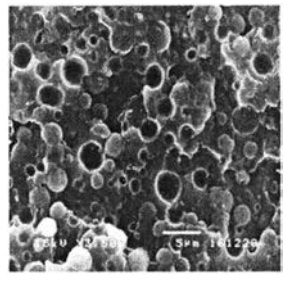

(a) PTT/HDPE : 80/20

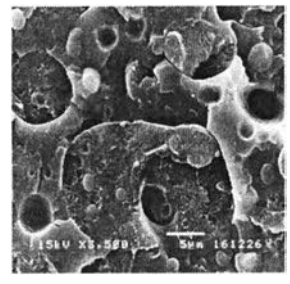

(b) PTT/HDPE : 60/40

Figure 4.1 SEM micrographs of the uncompatibilized PTT/HDPE blends at different ratio as (a) PTT/HDPE: 80/20 and (b) PTT/HDPE: 60/40

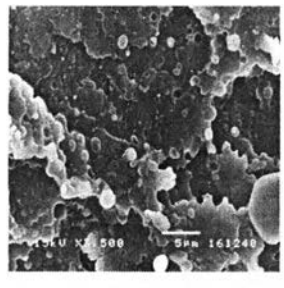

(a) 0.1 phr

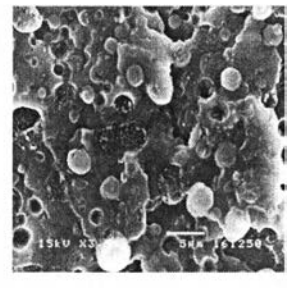

(b) 0.5 phr

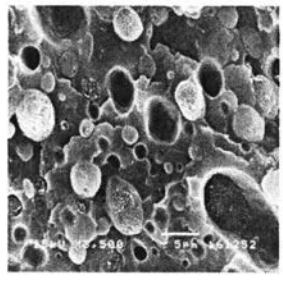

(c) 1 phr

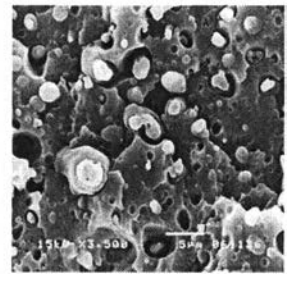

(d) 5 phr

Figure 4.2 SEM micrographs of compatibilized PTT/HDPE: 80/20 with different amount of MAH-g-HDPE.

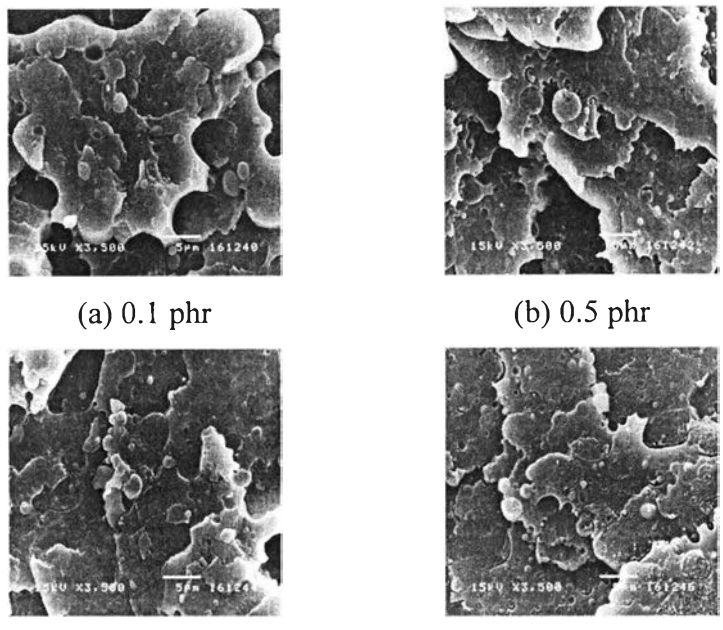

(a) 0.1 phr (b) 0.5 phr

(c) 1 phr (d) 5 phr

Figure 4.3 SEM micrographs of compatibilized PTT/HDPE: 60/40 with different amount of MAH-g-HDPE.

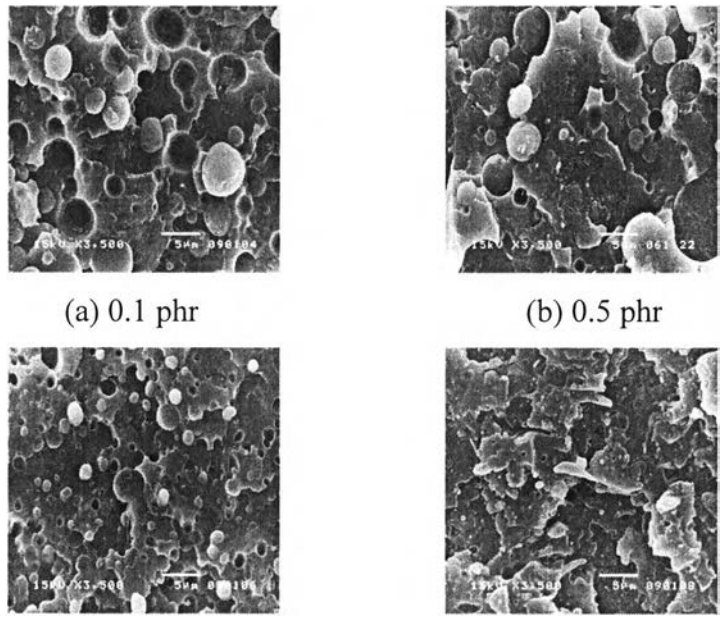

(a) 0.1 phr (b) 0.5 phr

(c) 1 phr (d) 5 phr

Figure 4.4 SEM micrographs of compatibilized PTT/HDPE: 80/20 with different amount of Na-EMAA.

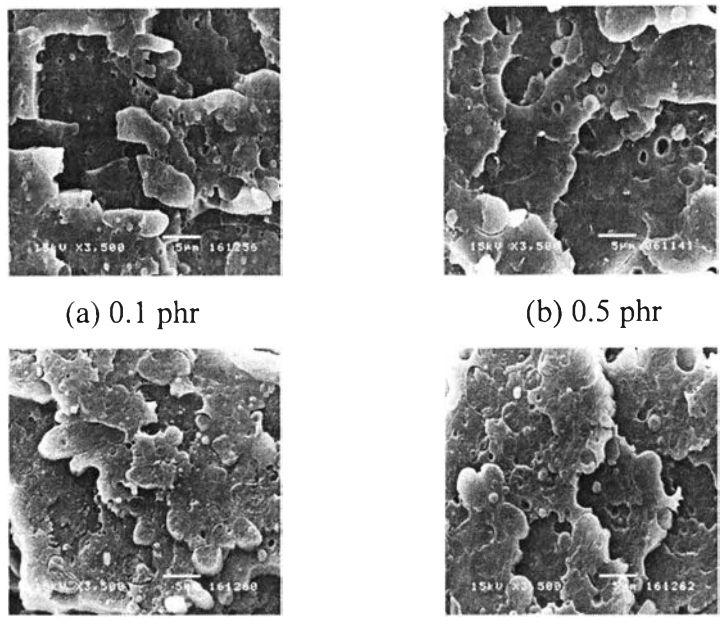

(a) 0.1 phr (b) 0.5 phr

(c) 1 phr (d) 5 phr

Figure 4.5 SEM micrographs of compatibilized PTT/HDPE: 60/40 with different amount of Na-EMAA.

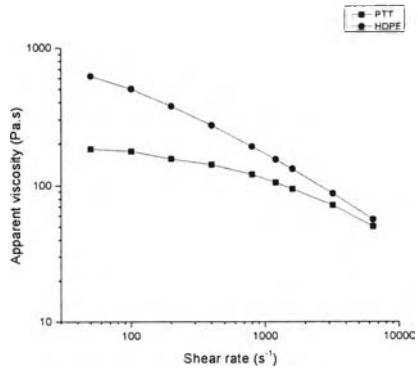

Figure 4.6 Melt viscosity of PTT and HDPE.

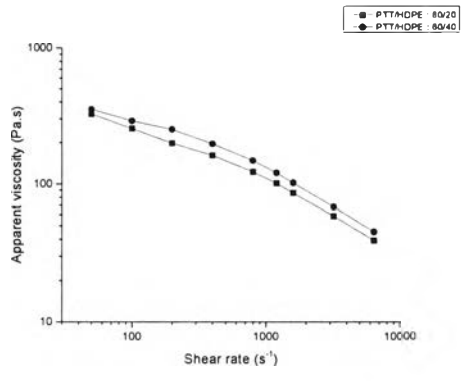

Figure 4.7 Melt viscosity of PTT/HDPE.

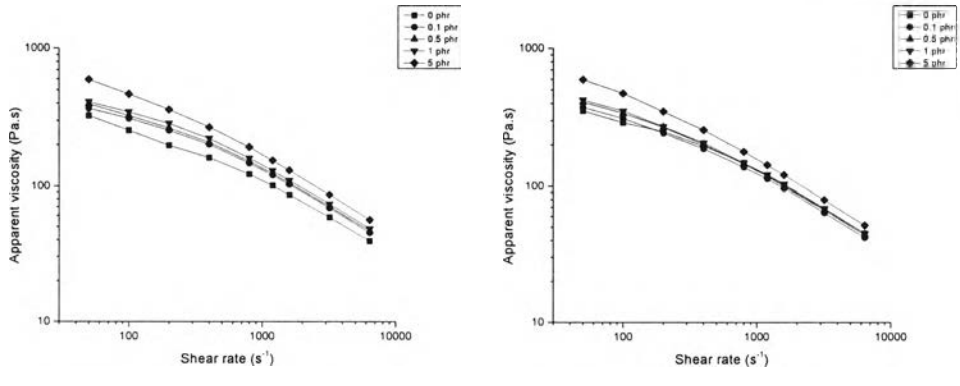

(a) (b)

Figure 4.8 Melt viscosity of PTT/HDPE: (a) 80/20 and (b) 60/40 blends with different amount of MAH-g-HDPE.

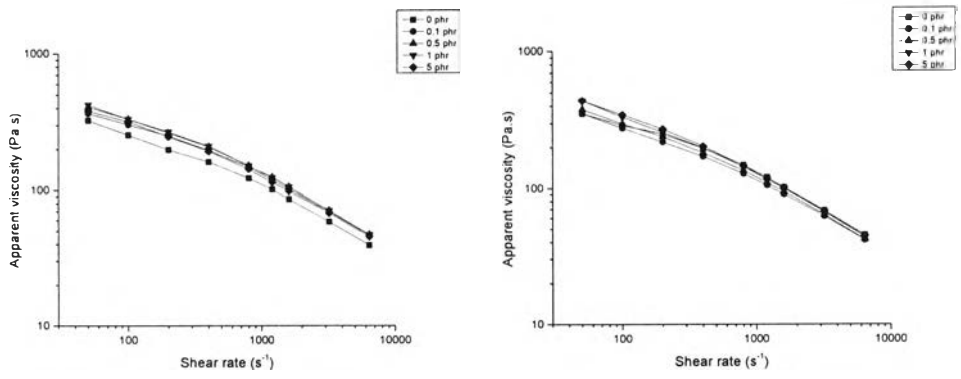

(a) (b)

Figure 4.9 Melt viscosity of PTT/HDPE: (a) 80/20 and (b) 60/40 blends with different amount of Na-EMAA.

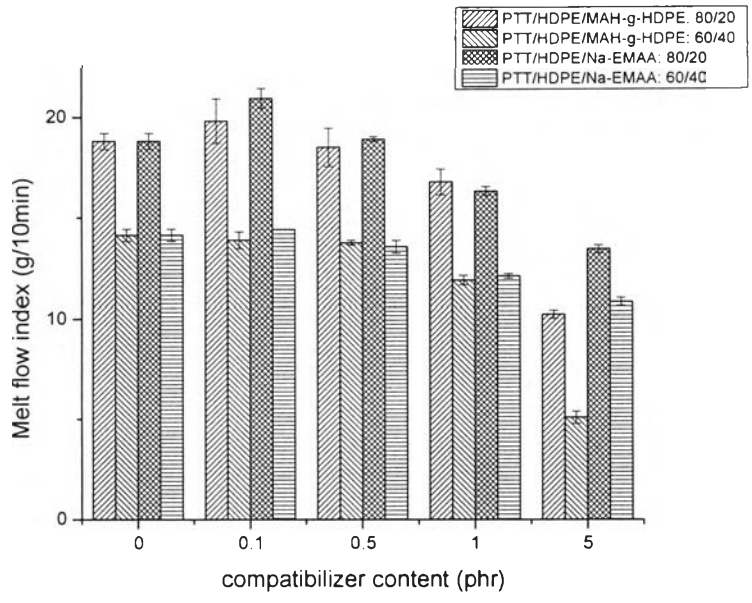

Figure 4.10 Melt flow index of PTT/HDPE blends with different compatibilizer contents.

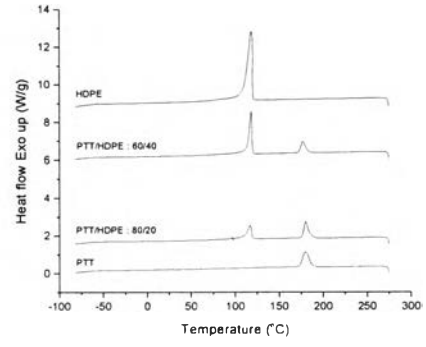

Figure 4.11 DSC thermograms at cooling scan of PTT/HDPE blends along with neat component.

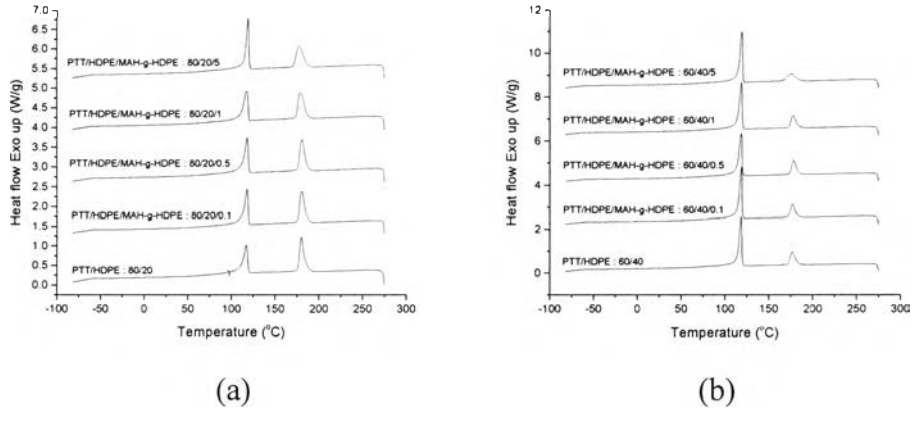

(a) (b)

Figure 4.12 DSC thermograms at cooling scan of PTT/HDPE (a) 80/20 (b) 60/40 blends with difference amount of MAH-g-HDPE.

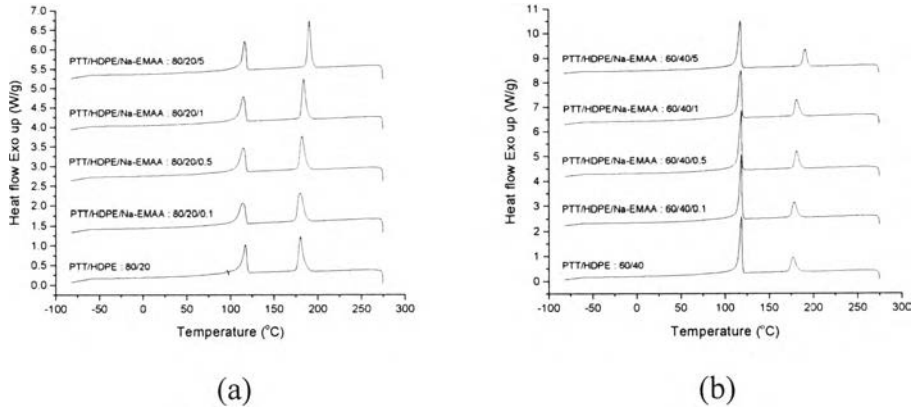

Figure 4.13 DSC thermograms at cooling scan of PTT/HDPE (a) 80/20 (b) 60/40 blends with difference amount of Na-EMAA.

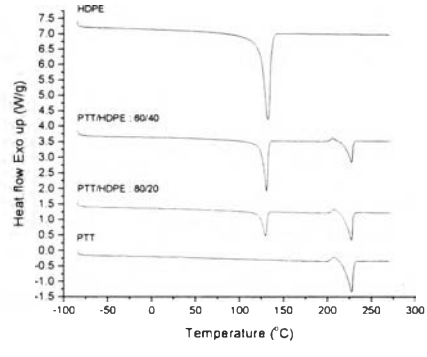

Figure 4.14 DSC thermograms at second heating scan of PTT/HDPE blends along with pure component.

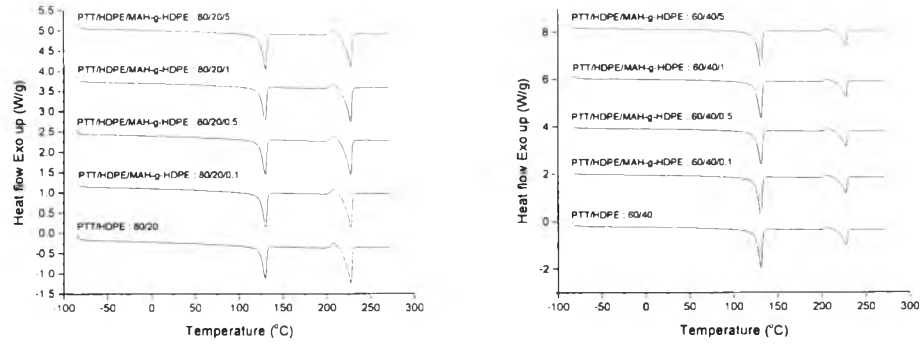

(a) (b)

Figure 4.15 DSC thermograms at second heating scan of PTT/HDPE (a) 80/20 (b) 60/40 blends with difference amount of MAH-g-HDPE.

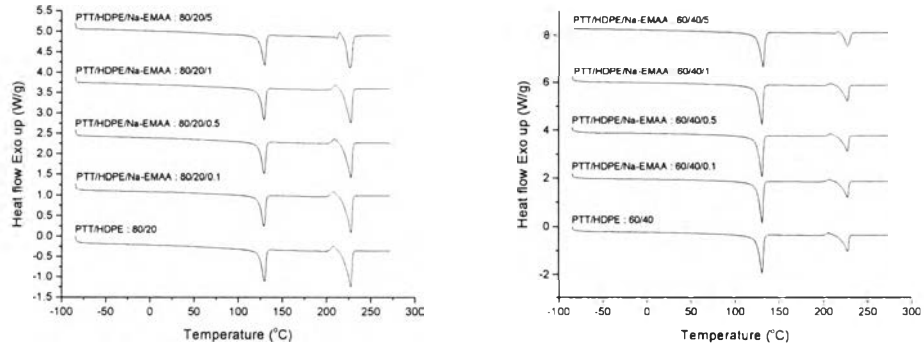

(a) (b)

Figure 4.16 DSC thermograms at second heating scan of PTT/HDPE (a) 80/20 (b) 60/40 blends with difference amount of Na-EMAA.

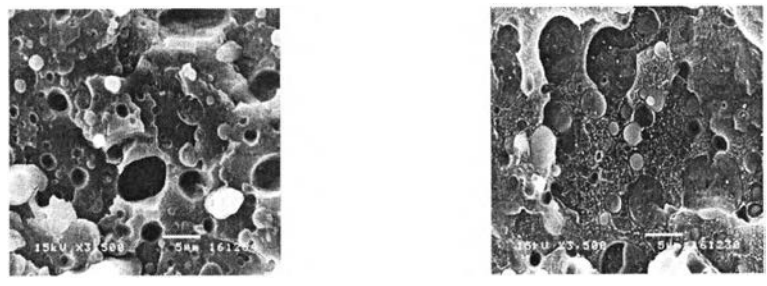

(a) PTT/LLDPE : 80/20 (b) PTT/LLDPE : 60/40

Figure 4.17 SEM micrographs of the uncompatibilized PTT/LLDPE blends at different ratio as (a) PTT/LLDPE: 80/20 and (b) PTT/LLDPE: 60/40

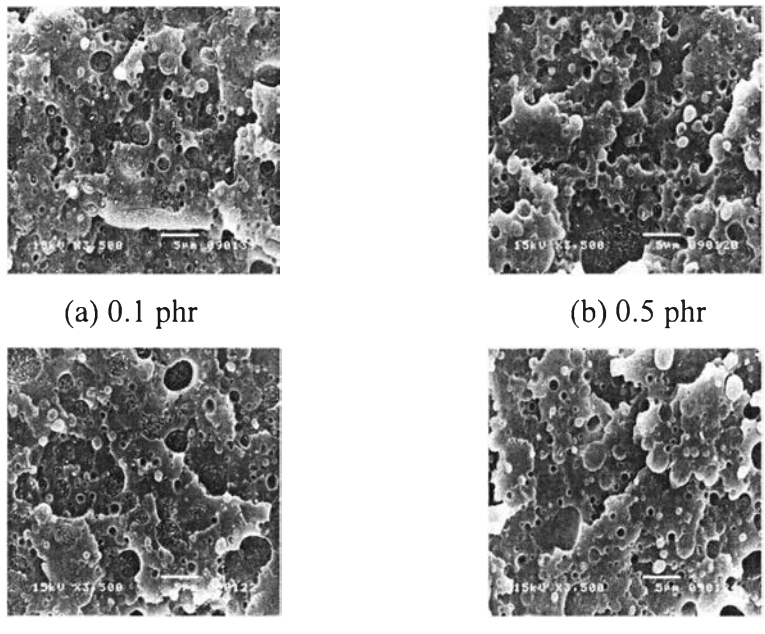

(a) 0.1 phr (b) 0.5 phr

(c) 1 phr (d) 5 phr

Figure 4.18 SEM micrographs of compatibilized PTT/LLDPE: 80/20 with different amount of MAH-g-HDPE.

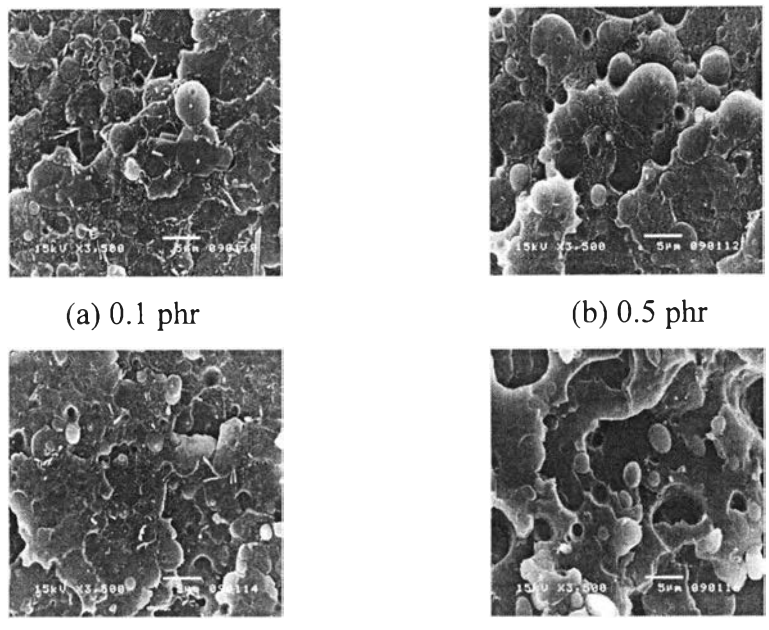

(a) 0.1 phr (b) 0.5 phr

(c) 1 phr (d) 5 phr

Figure 4.19 SEM micrographs of compatibilized PTT/LLDPE: 60/40 with different amount of MAH-g-HDPE.

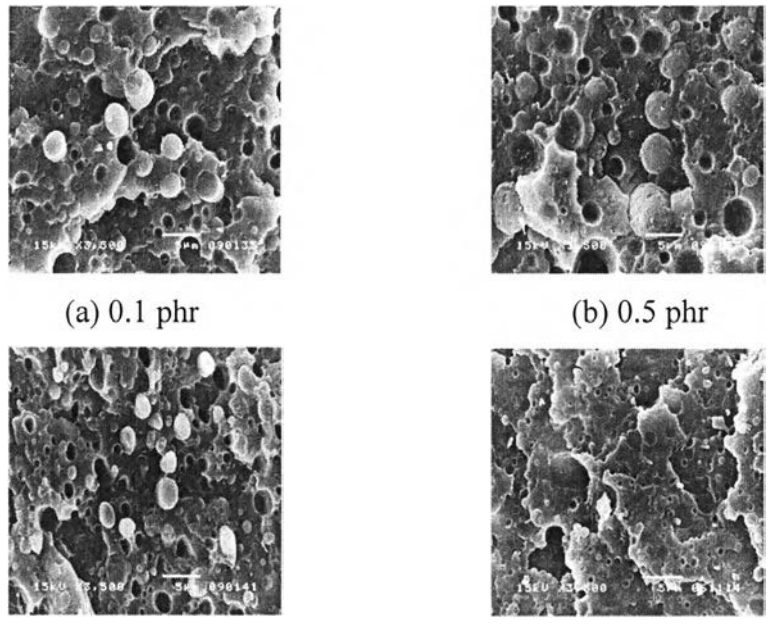

(a) 0.1 phr (b) 0.5 phr

(c) 1 phr (d) 5 phr

Figure 4.20 SEM micrographs of compatibilized PTT/LLDPE: 80/20 with different amount of Na-EMAA.

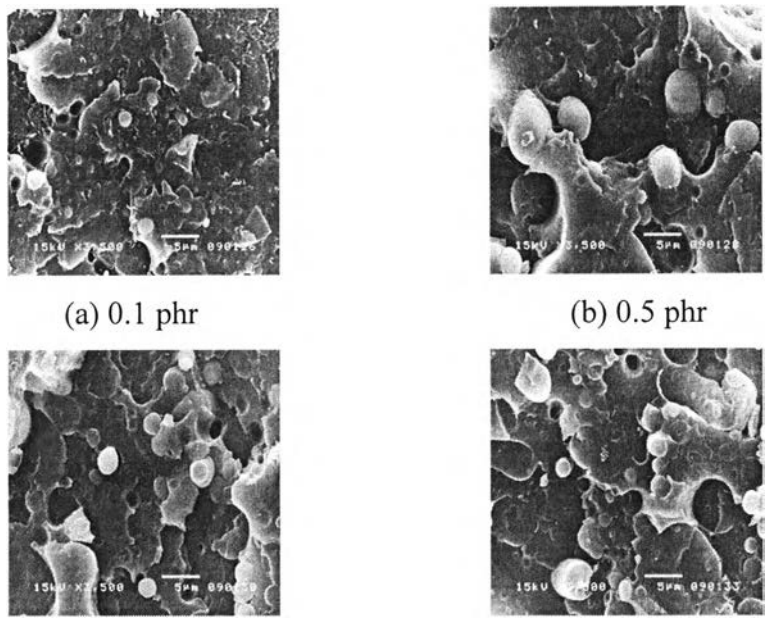

(a) 0.1 phr (b) 0.5 phr

(c) 1 phr (d) 5 phr

Figure 4.21 SEM micrographs of compatibilized PTT/LLDPE: 60/40 with different amount of Na-EMAA.

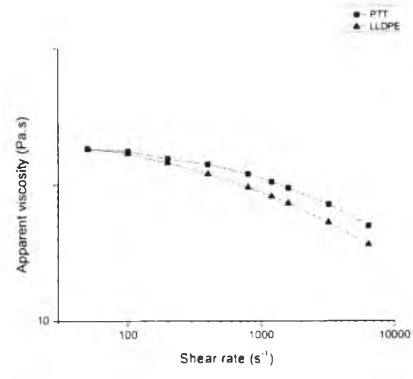

Figure 4.22 Melt viscosity of PTT and LLDPE.

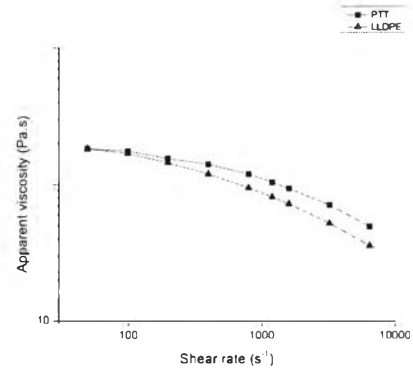

Figure 4.23 Melt viscosity of PTT/LLDPE blends.

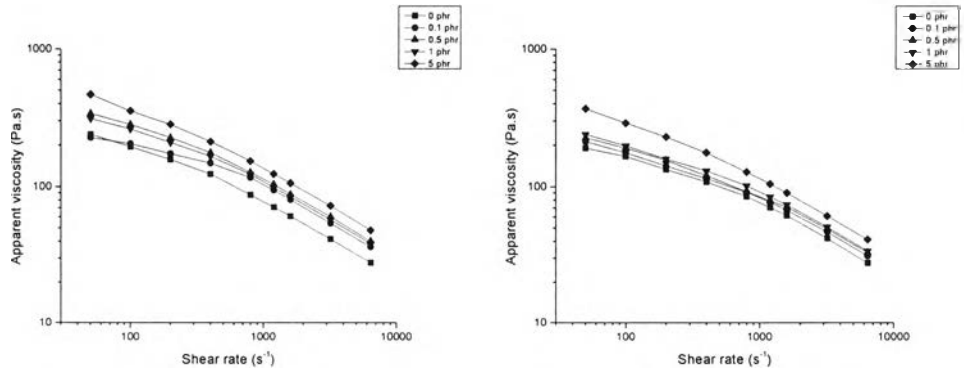

(a) (b)

Figure 4.24 Melt viscosity of PTT/LLDPE: (a) 80/20 and (b) 60/40 blends with different amount of MAH-g-HDPE.

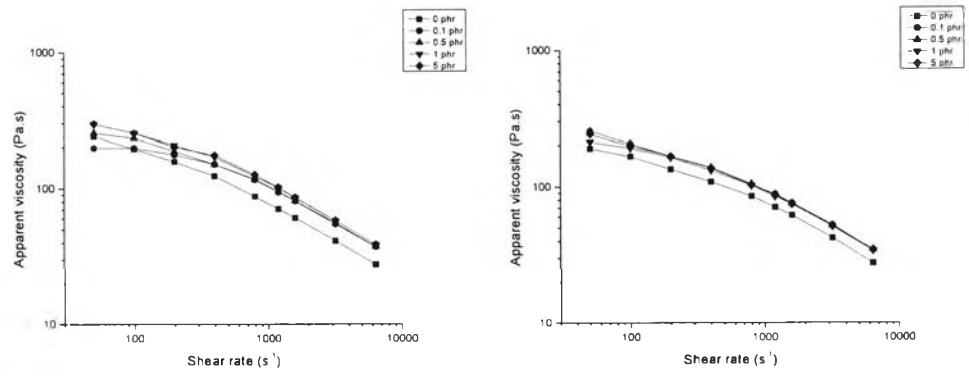

Figure 4.25 Melt viscosity of PTT/LLDPE: (a) 80/20 and (b) 60/40 blends with different amount of Na-EMAA.

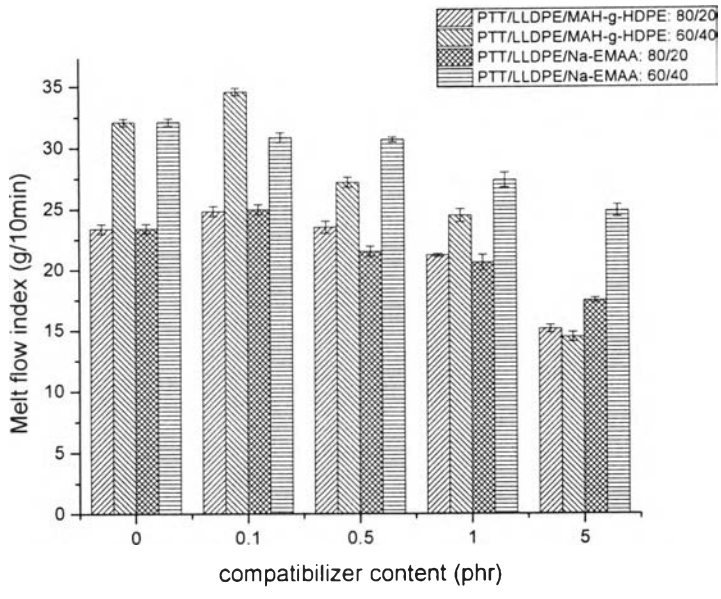

Figure 4.26 Melt flow index of PTT/LLDPE blends with different compatibilizer contents.

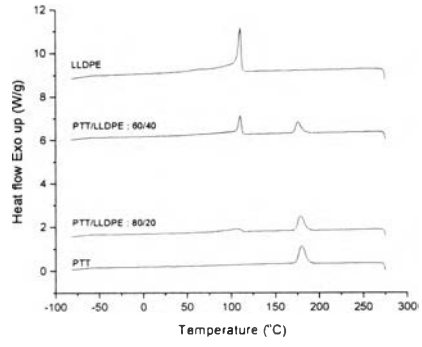

Figure 4.27 DSC thermograms at cooling scan of PTT/LLDPE blends along with neat component.

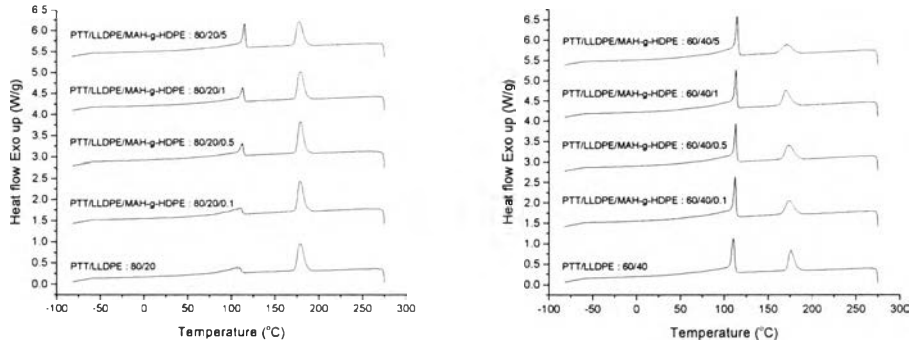

(a) (b)

Figure 4.28 DSC thermograms at cooling scan of PTT/LLDPE (a) 80/20 (b) 60/40 blends with difference amount of MAH-g-HDPE.

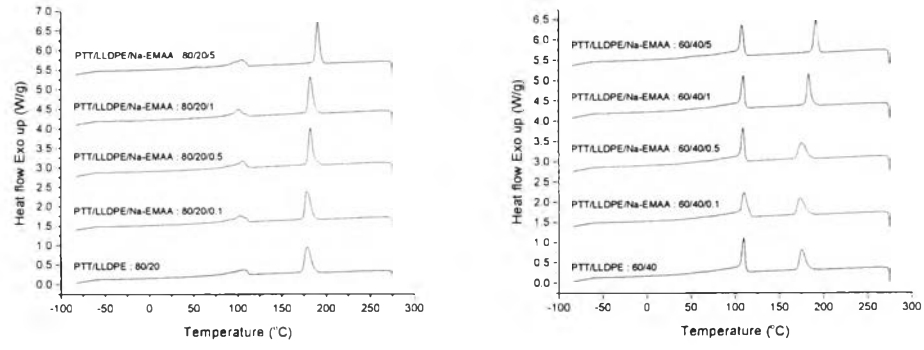

(a) (b)

Figure 4.29 DSC thermograms at cooling scan of PTT/LLDPE (a) 80/20 (b) 60/40 blends with difference amount of Na-EMAA.

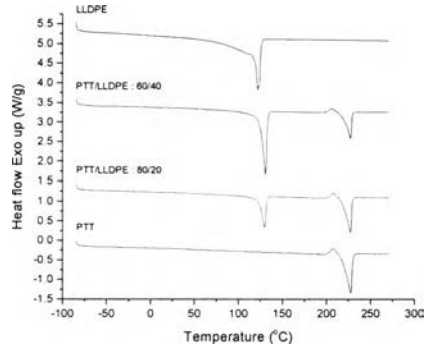

Figure 4.30 DSC thermograms at second heating scan of PTT/LLDPE blends along with pure component.

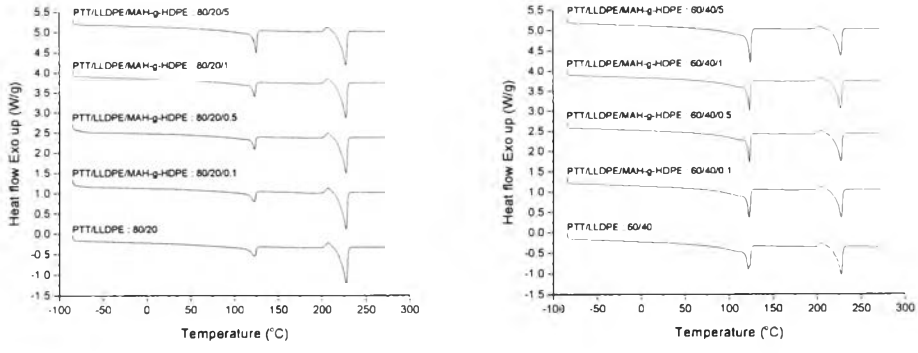

(a) (b)

Figure 4.31 DSC thermograms at second heating scan of PTT/LLDPE (a) 80/20 (b) 60/40 blends with difference amount of MAH-g-HDPE.

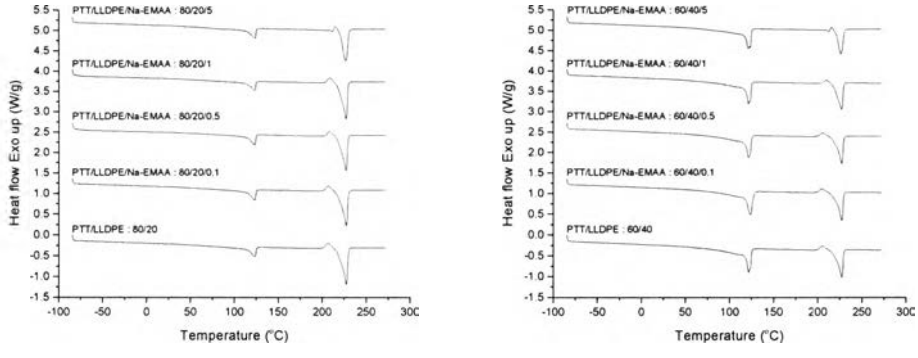

(a) (b)

Figure 4.32 DSC thermograms at second heating scan of PTT/LLDPE (a) 80/20 (b) 60/40 blends with difference amount of Na-EMAA.